

Material Modeling for Accuracy Improvement of the Springback Prediction of High-strength Steel Sheets

Tohru YOSHIDA*
Eiji ISOGAI
Shigeru YONEMURA

Akihiro UENISHI
Koichi SATO

Abstract

Improving the prediction accuracy of springback simulation are one of the most important problem because springback is major forming defect in sheet metal forming using high strength steel sheets. By applying the mixed hardening model by Lemaitre-Chaboche, which is possible to consider the Bauschinger effect under reverse loading path, prediction accuracy of springback were improved. And influences of material parameters of this model on springback deformation are investigated. To investigate the mechanism of the 3D springback, theoretical evaluation of simulation results before springback is carried out. It was found that 3D springback were reduced effectively by countermeasures obtained from that analytical results applied to the rear member model tests.

1. Introduction

Weight reduction for environmental considerations and enhanced collision safety are major current issues in the automotive industry, and as a solution for both, use of steel materials of higher strength for car bodies is increasing.¹⁾ The main problem with the use of high-strength steel sheets as compared with those of ordinary strength is its poor shape fixability due to springback. A common countermeasure against springback is to design forming dies that anticipate this behavior (springback compensation), but how much compensation is necessary is a difficult question, even for experienced die designers, and therefore actual field practice is largely based on trial and error.

On the other hand, accurate prediction of springback based on the simulation of forming, which has advanced remarkably in the last few years, would enable optimum die design with respect to springback compensation. An important point for forming simulations is how accurately the work hardening models used in springback analysis can reflect the yield stress decrease resulting from the de-

formation path (typically the Bauschinger effect). There have been some studies on the application of high-accuracy work hardening models to springback analysis.²⁻⁴⁾ Herein is presented a study on the effects of the material parameters on the accuracy of springback analysis using work hardening models that can take the Bauschinger effect into account. A factor analysis based on the change of material parameters due to higher material strength, the analysis results, and examples of countermeasures against springback are also discussed.

2. Accuracy Improvement of Springback Prediction Using Work Hardening Models that Consider the Bauschinger Effect

Springback is the elastic deformation of a steel sheet resulting from the release of stress that has accumulated in it during the stroke of a forming die down to the bottom dead center. For high-accuracy springback analysis, it is essential to correctly take into consideration the deformation path that the material sheet has undergone during the forming process. In a press forming process, in particular, a

* Chief Researcher, Dr., Forming Technologies R&D Center, Steel Research Laboratories
20-1, Shintomi, Futtu, Chiba 293-8511

steel sheet undergoes bending and unbending work when it enters the gap between the dies around a shoulder; during this process, the deformation mode changes from tension to compression on one side of the sheet, and from compression to tension on the other. **Fig. 1** shows the stress-strain relationship during a reverse loading test (in red) compared with the curve (in blue) generated from a simulation based on the isotropic hardening model, a commonly used work hardening model that does not take the Bauschinger effect into account. As can be seen in the figure, the section after load reversal of the stress-strain curve obtained from the test deviates significantly from that of the simulated curve. Because it is impossible to accurately calculate the stress distribution at the bottom dead center based on the isotropic hardening model, the accuracy of the springback prediction by this model is naturally poor.

Fig. 2 shows the characteristics of typical work hardening models used for forming simulations. According to the isotropic hardening model (a), the yield surface expands concentrically regardless of the mode of deformation, while according to the kinematic hardening model (b), the center of the yield surface shifts as deformation advances, and for this reason, this model can express the deformation condition where the amount of work hardening is different depending on the deformation mode. Thus, the latter model is known to be capable of reflecting the Bauschinger effect. In addition, as

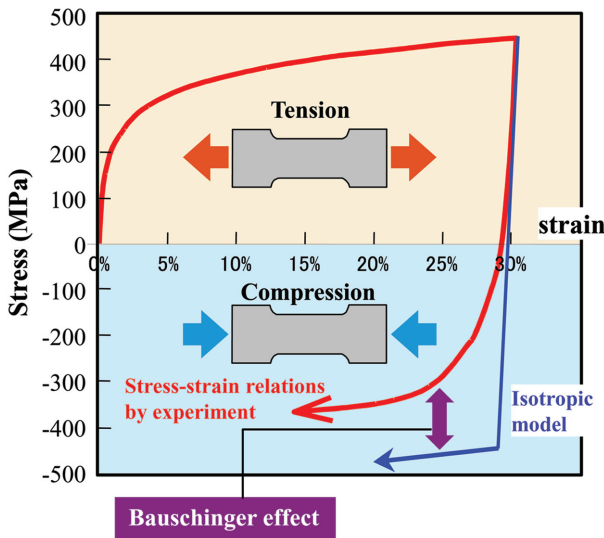


Fig. 1 Stress-strain relations under reverse deformations

shown in Fig. 2 (c), mixed hardening models that combine isotropic and kinematic hardening have been proposed. Specifically, the mixed hardening model proposed by Lemaitre-Chaboche (hereafter called the L-C model) is expressed as follows⁵⁾:

$$f = \sigma_e(\boldsymbol{\sigma}, \mathbf{X}) - R(\varepsilon_p) \quad (1)$$

$$R(\varepsilon_p) = Y + R_{sat}(1 - e^{-C_r \varepsilon_p}) \quad (2)$$

$$d\mathbf{X} = C_x X_{sat} d\varepsilon_p - C_x \mathbf{X} d\varepsilon_p \quad (3)$$

where $\sigma_e(\boldsymbol{\sigma}, \mathbf{X})$ is the equivalent stress, ε_p is the equivalent plastic strain, \mathbf{X} is the back stress, $R(\varepsilon_p)$ is the isotropic hardening stress, Y is the yield stress, R_{sat} and C_r are the material parameters for the isotropic hardening model representing the critical stress and work hardening ratio, respectively, under infinite strain, and X_{sat} and C_x are the material parameters for the kinematic hardening model. When $R_{sat} = 0$, this model is equivalent to the kinematic hardening model, and when $X_{sat} = 0$, it is equivalent to the isotropic hardening model. The number of material parameters used for this model is five.

In order to examine the effects of the isotropic, kinematic, and mixed hardening models on the results of a springback simulation using the L-C model, the parameters were defined such that the values of the stress calculated according to the three hardening models were the same before, but different after, load reversal. **Table 1** shows the parameter values thus determined, and **Fig. 3** depicts the stress-strain relationship after the load reversal. According to the isotropic hardening model, the stress after load reversal is always the same as the stress before it in terms of absolute value, while a stress decrease after load reversal is clear in the kinematic and mixed hardening models. For the springback analysis, a simulation of hat-shape bending was conducted by applying the above parameter values and based on the die dimensions given in **Fig. 4**.

In the hat-shape bending test, the occurrence of wall warping depends largely on the fitting of the material sheet with the die shoulder. Based on this fact, the die shoulder radius R was changed in

Table 1 Material parameters for stress-strain relations in reverse loading path

	Y (MPa)	R_{sat} (MPa)	C_r	X_{sat} (MPa)	C_x
Isotropic hardening	260	340	9	0	0
Kinematic hardening	260	0	0	340	6.5
Mixed hardening	260	240	5	100	20

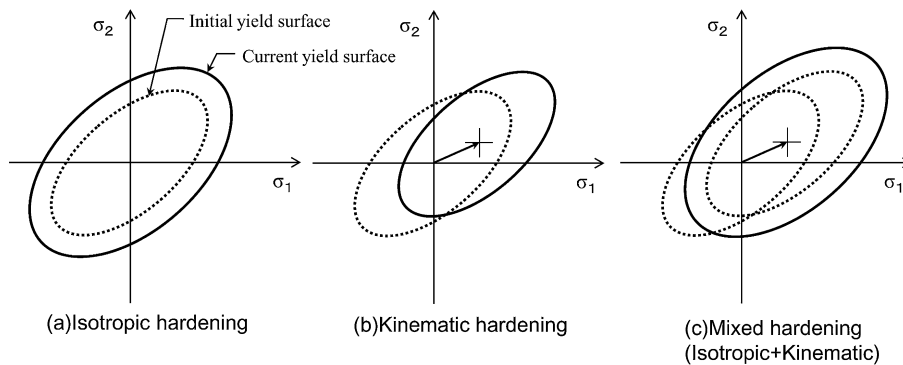


Fig. 2 Schematic illustration of work hardening models

relation to the sheet thickness t , and the effects of the ratio R/t was investigated. Fig. 5 shows the wall warping obtained through forming and springback analyses. When R/t was 3 or less, the curvature of the wall warping was larger in the mixed hardening model than in the isotropic hardening model. When R/t was approximately 2 in particular, the wall curvature for the isotropic hardening model became negative, indicating internal warping. When the ratio was 4 to 5 or more, in contrast, the curvature in the isotropic hardening model was larger than that in the mixed hardening model. Thus, the magnitude of the relationship between the wall curvature estimated according to the different hardening models is inversely proportional to the value of R/t . This result is presumably due to the different yielding behaviors after load reversal, which lead to different fittings of the material sheet with the die shoulder. It should be noted, therefore, that the change in wall warping is not determined solely by the work hardening model used for the simulation.

In addition, partly because of the difficulties associated with reverse loading tests for steel sheets, a method for obtaining the material parameters for use as input in the constitutive equations for the materials has not been well established. In fact, regarding the

uniaxial deformation test under reverse tension-compression loading, there have been some proposed methods for suppressing buckling during compression,^{6,7)} but even with these methods, the measurement over large-deformation ranges is not easy with high-strength specimens. In the shear test, in contrast, buckling and fracture are unlikely to occur, even under large plastic deformation, and reverse loading over large deformation ranges corresponding to bending and unbending is applicable. Therefore, the shear test is more suitable for the measurement of work hardening behavior, including the Bauschinger effect, over wide ranges of strain.⁴⁾ Fig. 6 shows the results of reverse loading tests for 590-MPa high-strength steel sheet specimens using the simple shear method, along with the calculated results for the mixed hardening model obtained using these test results. The graph clearly shows good agreement between the experimental and calculated results from the transitory softening region to the

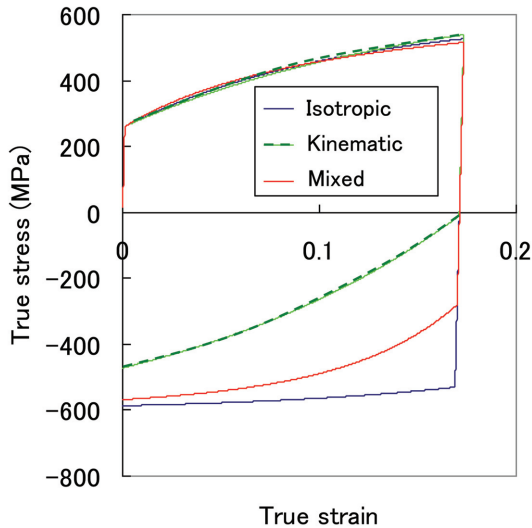


Fig. 3 Stress-strain relations of each work hardening models in reverse loading path

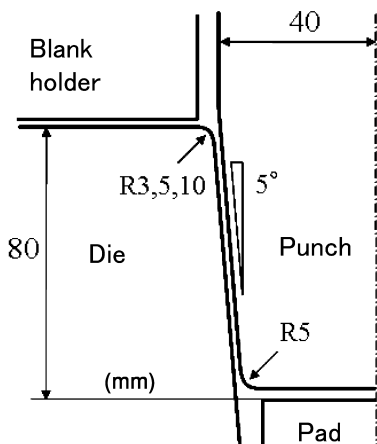


Fig. 4 Tool dimensions of hat shape bending

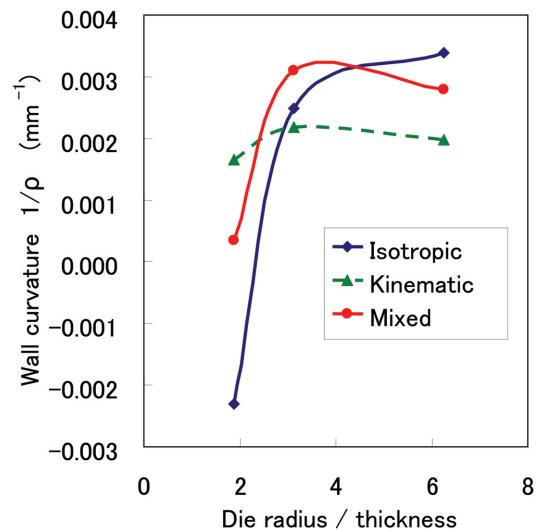


Fig. 5 Influence of die radius on wall curvature after springback in hat shape bending

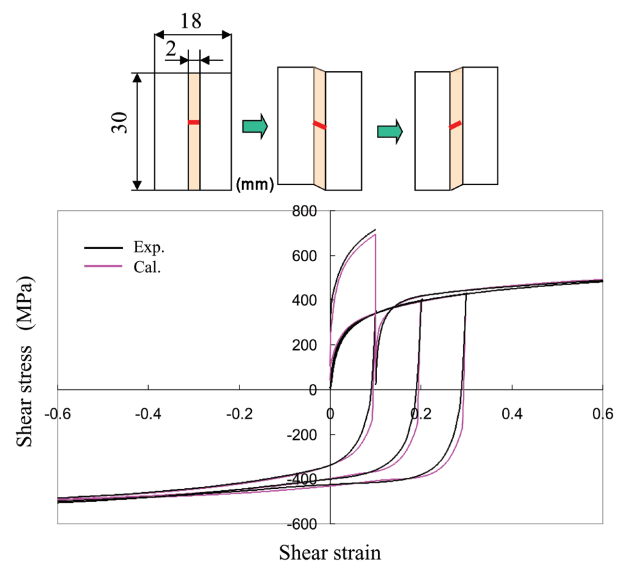


Fig. 6 Comparison of stress-strain relations between experiment and calculation results by simple shear tests

permanent softening region.

3. Change in the Bauschinger Effect Due to Higher Material Strength and Shape Fixability

The problem of poor shape fixability is more conspicuous with high-strength materials, and for this reason, it is important to understand how high material strength influences the Bauschinger effect. Therefore, a systematic investigation of solid-solution hardening, a basic steel strengthening method, was conducted. Solid-solution-hardened specimen sheets of different strengths were prepared by changing the Mn and Si content in an interstitial-free steel, and these materials were subjected to tensile and simple shear tests. **Table 2** compares the specimens in terms of the increase in the flow stress due to solid solution hardening as measured by the tensile test; here, Steel A is the reference specimen. The Bauschinger effect was seen in all of the specimens at reverse loading using the simple shear test. The parameters for the L-C model were defined based on these test results.

The parameters thus defined are given in Table 2. Here, the values of C_r and C_x as defined according to the test results for Steel A were used for all of the other specimens. Even so, the simulations agreed well with the test results, which seems to indicate that, as far as these specimens are concerned, the elementary processes that govern softening after load reversal do not change significantly. In addition, the parameters defined according to the test results were compared with the increase in flow stress due to solid solution hardening (see Fig. 7). It was found that the increase in the flow stress due to solid solution hardening changed substantially in a linear fashion with respect to the parameters of the L-C model. The slope of the linear relationship, however, was different for each parameter. Spe-

cifically, the ratio X_{sat}/R_{sat} was found to increase with increasing strength, which indicates that kinematic hardening is more conspicuous in solid-solution-hardened materials. Microscopically, kinematic hardening is considered to result from interactions directional to mobile dislocations, such as elastic stress fields resulting from dislocations accumulated in obstacles.

Springback analysis was conducted using the material parameters in Table 2. Here, the values of R_{sat} and X_{sat} of Steel A' were determined such that the ratio of the kinematic hardening component (X_{sat}/R_{sat}) was the same as that for Steel C. Springback evaluation was conducted assuming that $1.8 \times 280 \times 100$ mm specimen sheets were subjected to hat-shaped bending (with two vertical walls) using dies with a width of 80 mm and a shoulder radius of 5 mm. **Fig. 8** shows the width opening (ΔW_1) on one side. As has been previously observed, the springback amount increased as the material strength increased. However, Steel A', which had the same strength as that of Steel A and the same value of X_{sat}/R_{sat} as that of Steel C, tended to exhibit a larger wall opening with a low blank holding force (BHF) compared to that of Steel A. This result is presumably because the Steel A and A' specimens deformed differently at the die shoulders because of their different flow stresses during bending and unbending. As stated above, it became clear that, although the amount of springback was predominantly influenced by the material strength, it was also affected by the ratio of the kinematic hardening component (X_{sat}/R_{sat}).

4. Application of the Springback Simulation and Factor Analysis

There are no all-purpose measures to prevent three-dimensional forming problems such as torsion, camber, etc. from occurring in

Table 2 Increase in flow stress of materials due to solid-solution hardening and material parameters of Lemaitre-Chaboche model

	$\Delta\sigma$ (MPa)	C_r	R_{sat} (MPa)	C_x	X_{sat} (MPa)	Y (MPa)	X_{sat}/R_{sat}
Steel A	-	6.24	246	142	52	81	0.21
Steel B	41		256		59	110	0.23
Steel C	219		334		105	174	0.31
Steel A'	-		222		69	81	0.31

$\Delta\sigma$: Increase in flow stress

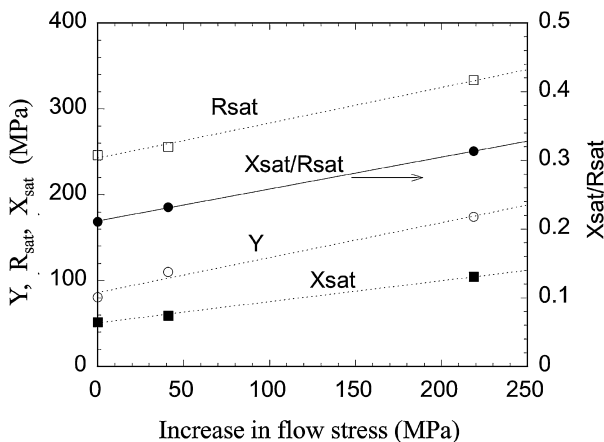


Fig. 7 Lemaitre-Chaboche model parameters vs. the increase in flow stress due to solid-solution hardening

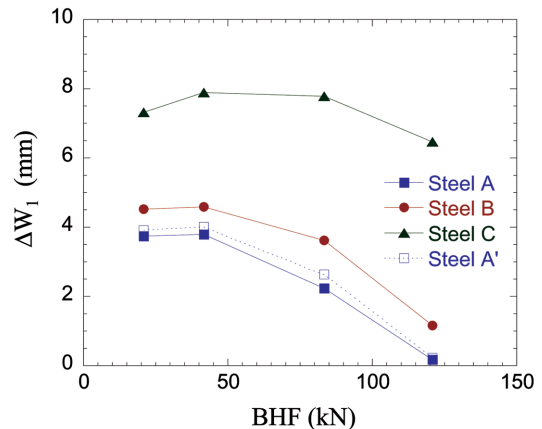


Fig. 8 Opening width in vertical wall side (ΔW_1) vs. blank holding force (BHF)

field practice due to poor shape fixability. Therefore, a set of dies modeling a rear member part with curvatures in the in-plane and punch-stroke directions was used to verify the accuracy of the springback analysis regarding torsion and camber, to investigate the mechanisms of these problems, and to study possible countermeasures.⁸⁾

Specimen sheets of strengths ranging from 270 to 980 MPa were formed using the dies for the rear member part shown in Fig. 9, and the torsion angle θ_{AB} and the camber δ_B between sections A and B were measured. The measurement results made it clear that both θ_{AB} and δ_B increased as the material strength increased, and that the sheet thickness and lubrication also had significant effects. Next, using the isotropic hardening model and the mixed hardening model (the L-C model), forming and springback analyses were conducted with respect to the forming of a 1.2 mm-thick 980 MPa strength specimen sheet into the same rear member part.

Fig. 10 shows the error distribution maps demonstrating the distances between points in the design of the subject rear member part using computer aided design (CAD) and the corresponding points in the calculated springback results. Additionally, Fig. 11 compares the simulated and experimentally-obtained shapes of section B. The simulation result based on the mixed hardening model agreed well with the test results in terms of the torsion and the tendency of the upward turn of the flanges. In the simulation based on the isotropic hardening model, in contrast, the torsion was excessively large and the upward turn of the flanges was different from the test results. These findings seem to indicate that use of a work hardening model taking the Bauschinger effect into consideration improves the simulation accuracy regarding wall opening, and as a result, the accuracy of the torsion is also improved. Thus, use of a hardening model taking the Bauschinger effect into consideration proved effective at predicting three-dimensional shape fixability problems occurring with parts such as the one studied here.

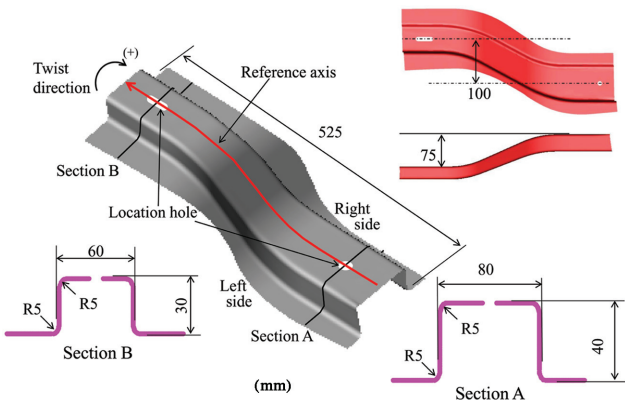


Fig. 9 Detail profile of the rear member parts

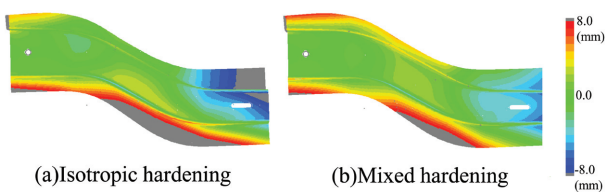


Fig. 10 Contour map of differences between springback simulation results and CAD shape

Because springback is directly caused by the internal stress imposed on the material during press forming work, in order to develop countermeasures, it is important to mechanically evaluate the causes using the stress distribution at the bottom dead center of a forming stroke, which is obtainable through forming simulation. Therefore, a method⁹⁾ for obtaining the torsion by evaluating the torque resulting from an internal stress was applied to the rear member part model. Assuming that the longitudinal direction of the part is the reference axis (t direction), the torque T about the center t of an assessment section perpendicular to the reference axis is given by the following equation:

$$T(t) = \int (qr_c \sin \theta + M_{ts}) ds \quad (4)$$

where q is the in-plane shear stress, r_c is the vector of the point of action with respect to the center t, θ is the angle between r_c and the tangential vector of the section, and M_{ts} is the twisting moment. By applying this analysis method to the stress distribution at the bottom dead center obtained through forming simulation, it is possible to estimate the distribution of the in-plane shear stress at different positions, as well as the twisting moment, the torque, and the torsion angle in the section in question. In order to clarify the positions of the formed part where the twisting moment was significantly large, the part was divided into five portions, namely the web, the walls, and the flanges, and the twisting moment was estimated for each section. Fig. 12 shows the results. This analysis made it clear that the twisting moment was large in the vertical walls, and particularly, the torsion originated from a portion of the wall near the curve, where

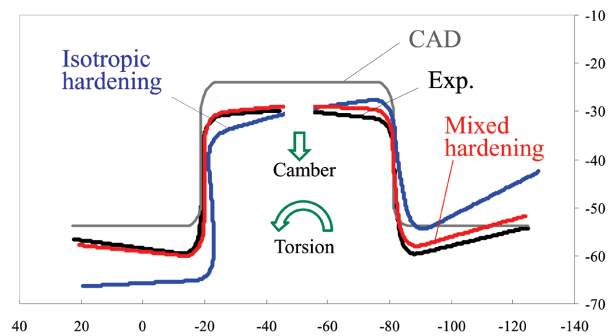


Fig. 11 Comparison of sectional shapes on B section

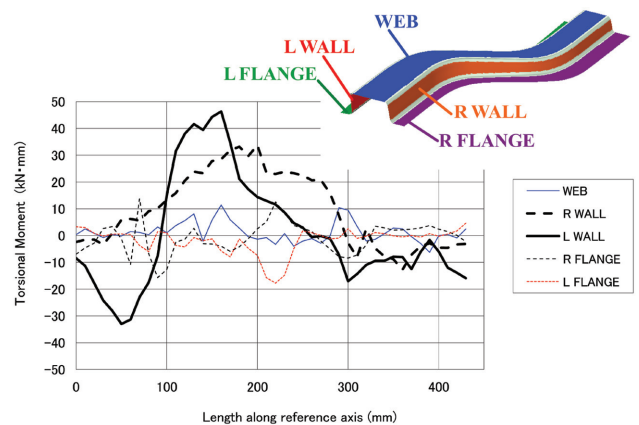


Fig. 12 Torsion moment distributions on each area of rear member

both the flanges and walls underwent compressive deformation.

5. Countermeasures against Springback and Effect Verification through Testing

From the torque estimation described in Section 4, it was clear that the twisting moment was large in the vertical walls, and was largest in the portion of the walls near the large-width end, where heavy shrink flanging and elongation flanging were applied. Based on this finding, two countermeasures against the forming problem that disperse or reduce the stress in the affected portions were studied: (1) partial beads; and (2) width reduction. High-strength steel sheets (980 MPa, 1.2 mm-thick) were used as the specimens for the tests designed to verify the effects of these measures.

(1) Partial beads

In order to disperse and reduce the longitudinal stress imposed on the vertical walls that caused the torsion, beads were formed along the corners in the portions where shrink flanging and elongation flanging occurred, and the effect of their presence was examined. The tools (dies, punch and blank holders) were divided into sections, and grooves/protrusions for the beads were formed in some of them so that the arrangement of the beads could be changed as desired by changing the sections. As can be seen in Fig. 13, the beads were designed to have a round section 5 mm in radius (on the die side) and 2 mm in height. When the beads were formed in the shrink flanging and elongation flanging regions near the large width end (based on the results of the factor analysis in Figure 12), they exhibited significant effects, particularly when they were formed in the shrink flanging regions, and the twisting direction was reversed. Beads at different positions of the part proved effective at decreasing the camber. It is assumed that the partial beads controlled the residual stress in specific portions of the walls and the flanges, and consequently, the overall balance of the twisting moment was improved, leading to a decrease in the torsion angle and the camber.

(2) Width reduction

As another countermeasure against the forming problems, width reduction was attempted. In this method, as shown in Fig. 14, the sections where shrink flanging or elongation flanging are likely to occur were formed a little wider in the first step, and then reduced to the originally-designed widths in the second step. The tool sections

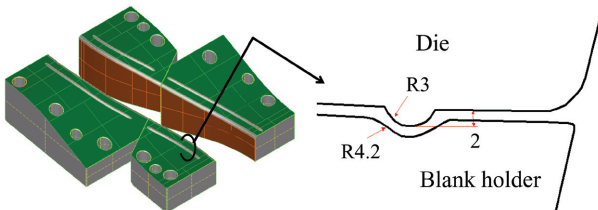


Fig. 13 Schematic of tool blocks and section shapes of partial bead

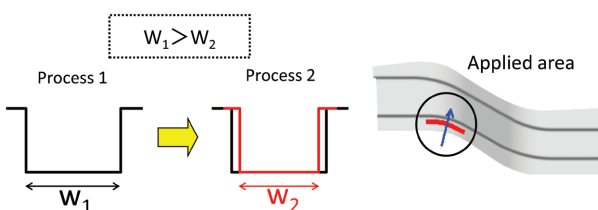


Fig. 14 Schematic of width reduction and applied area

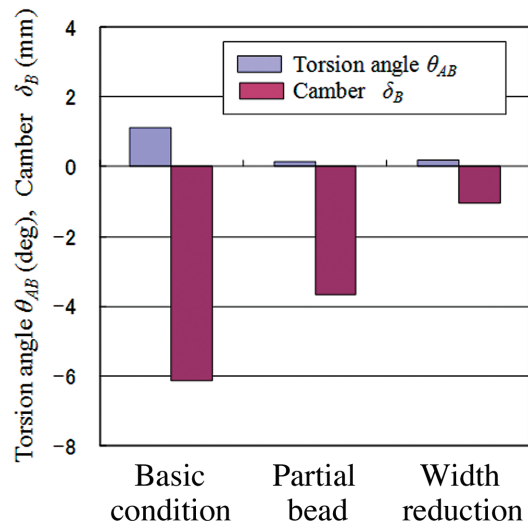


Fig. 15 Results of effects for reducing 3D spring-back by countermeasures (980MPa high strength steel, 1.2mm)

for the first step were prepared such that the curvature of the edges for the portions in question was modified from that of the tool sections for the second step, which were prepared according to the designed shape. The width reduction amount was set at 2 mm. From the results of this test, it became clear that the width reduction of the large-width end portion where elongation flanging was likely to occur proved effective in decreasing both the torsion and the camber.

Fig. 15 shows the effects of the measures to rectify the forming problems obtained in the cases where they proved most effective. These results indicate that it is possible to adequately control the residual stress and avoid forming problems by forming partial beads or partially reducing the width during forming. It also became clear, however, that the effects of these measures were different depending not only on the position where they were applied, but also their combined use. Therefore, it is essential to clarify the related factors and study the effects of each measure thoroughly before actually applying them.

6. Closing

Springback simulation that is essential for solving the shape fixability problems in the forming process for high-strength steel sheets has been discussed. With respect to work hardening models, it was found that the simulation accuracy could be improved by applying the Lemaitre-Chaboche mixed hardening model, thus strictly taking into consideration the deformation characteristics of steel sheets under reversing loads. The material parameters for specimens of different strengths were also measured, and the effects of the parameters on the springback prediction were identified. In addition, it became clear through tests that a factor analysis method making use of the simulation results could define measures for rectifying three-dimensional shape fixability problems, such as the torsion and camber. These methods are expected to be effective in solving problems in the forming of ultra-high-strength steel sheets, and thus expand the application of these materials to machine parts.

The Japanese manufacturing industries are facing tough competition from overseas counterparts, and in such a situation, they are required to develop new products of higher performance in shorter periods and at lower costs. In order to find an optimum solution for

these complex requirements, an overall approach covering aspects of the materials, processes, and structures is essential, and for rational and efficient practical implementation of such an approach, computer aided engineering (CAE) is indispensable. Therefore, the development of elementary CAE technologies that can adequately handle new materials and manufacturing processes is important, and thus it is necessary to continue pursuing more advanced analysis methods.

References

- 1) Sato, A.: J. Japan Society for Technology of Plasticity. 46 (534), 548 (2005), for example
- 2) Yoshida, F., Uemori, T.: Int. J. Plasticity. 18, 661 (2002)
- 3) Isogai, E., Yoshida, T., Hiwatashi, S., Hashimoto, K., Kuriyama, Y.: Proc. 57th Japanese Joint Conference for the Technology of Plasticity. 2006, p. 251
- 4) Suzuki, N., Hiwatashi, S., Uenishi, A., Kuwayama, T., Kuriyama, Y., Lemoine, X., Teodosiu, C.: J. Japan Society for Technology of Plasticity. 46 (534), 636 (2005)
- 5) Chaboche, J. L.: Int. J. Plasticity. 7, 661 (1991)
- 6) Uemori, T., Fujiwara, K., Okada, T., Yoshida, F.: J. Japan Society for Technology of Plasticity. 42 (480), 64 (2001)
- 7) Kuwabara, T., Morita, Y., Miyashita, Y., Takahashi, S.: J. Japan Society for Technology of Plasticity. 36 (414), 768 (1995)
- 8) Yoshida, T., Sato, K., Isogai, E., Hashimoto, K., Kuriyama, Y., Ito, K., Uemura, G.: Proc. 59th Japanese Joint Conference for Technology of Plasticity. 2008, p. 377
- 9) Kondoh, T., Ito, K., Uemura, G., Mori, N.: Proc. 2006 Japanese Spring Conference for the Technology of Plasticity. 2006, p. 113



Tohru YOSHIDA
Chief Researcher, Dr.
Forming Technologies R&D Center
Steel Research Laboratories
20-1, Shintomi, Futtsu, Chiba 293-8511



Koichi SATO
Senior Researcher, Dr.
Nagoya R&D Lab.



Akihiro UENISHI
Senior Researcher, Dr.
Forming Technologies R&D Center
Steel Research Laboratories



Shigeru YONEMURA
Senior Researcher, Dr.Eng.
Kimitsu R&D Lab.



Eiji ISOGAI
Senior Researcher
Hirohata R&D Lab.